TRANSACTIONS ON ELECTROMAGNETIC SPECTRUM

Analysis of a Compact UWB Antenna with Integrated Band-Notched Feature for Wireless Body Area Network Applications

Sammy O. Oladiran[1*], **Kazeem B. Adedeji**[2]

[1]Department of Information and Communication Technology, School of Electrical Systems Engineering, Federal University of Technology Akure, Ondo State, Nigeria, sooladiran@futa.edu.ng

[2]Department of Electrical and Electronics Engineering, School of Electrical Systems Engineering, Federal University of Technology Akure, Ondo State, Nigeria, Email: kezman0474@yahoo.com, kbadedeji@futa.edu.ng

*** Corresponding author's e-mail address:** sooladiran@futa.edu.ng

Received: 31 August 2025
Revised: 12 November 2025
Accepted: 5 December 2025

Research Article
Vol. 5 / No. 1 / 2026
Doi: 10.65819/tes.2026.v5i1.57

Abstract: This paper presents an analysis of a compact band-notched ultra-wideband antenna intended for Wireless Body Area Network applications. The antenna operates between 3.4 GHz and 12.9 GHz with notched frequency using H and U slots on the patch and feedline for notching 6.5 GHz – 7.9 GHz band. By employing a genetic algorithm, the antenna dimensions were refined to obtain a compact semi-circular configuration with overall dimensions of 26 mm × 27 mm and a 12 mm radius. A reduction in the specific absorption rate was achieved by integrating a defected ground structure along with rectangular slots into the antenna design. The antenna performance was assessed using several key antenna parameters. According to the simulation outcomes, the antenna achieves a return loss below −10 dB from 3.4 GHz to 12.9 GHz and provides an average gain of 6.4 dBi. Also, the developed antenna showed a significant improvement in SAR reduction to a level of 0.8 W/kg averaged over one gram of tissue, which is within the safe limits of the Federal Communications Commission (FCC) for low-power devices and therefore suitable for WBAN applications. In addition, the antenna demonstrates effective impedance matching. The average Poynting value of 4.09 W/m^2, which is evenly distributed over the patch and the feedline of the antenna, revealed a uniform radiated power density of the antenna. This value is 29.5% less than the safe limit announced by the FCC.

Keywords: Antenna, Frequency notch, Specific absorption rate, UWB, WBAN.

Cite this paper as: Oladiran SO., Adedeji KB., Analysis of a Compact UWB Antenna with Integrated Dual-Band Notch Features for Wireless Body Area Network Applications. Transactions on Electromagnetic Spectrum. 2026; 5(1): 1-11, Doi: 10.65819/tes.2026.v5i1.57

1. INTRODUCTION

In recent years, wireless communication technologies have gained increasing interest for the development of remote human body monitoring systems. Without interfering with day-to-day activities, WBAN can be used to monitor physical activity and chronic health. For real-time transfer, this requires fast speed, low power consumption, and larger bandwidth connectivity [1, 2]. A WBAN tracks the activities of the human body using a variety of small, independent sensors. As illustrated in Figure 1, positioning these sensors on the patient's body enables remote health monitoring of physiological parameters such as blood pressure, body temperature, heart rate, and blood glucose levels.

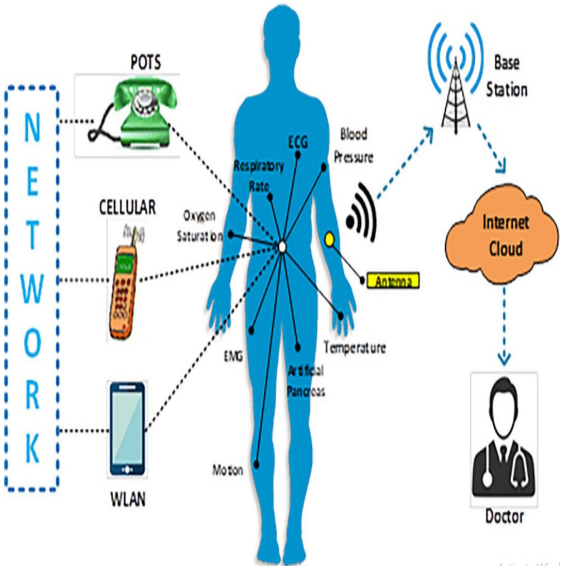

Figure 1. WBAN application [3].

The sensors for the WBAN can be implanted or wearable on human body. Both implanted and wearable WBANs are feasible with the aim of safeguarding people's health. This is accomplished by using body sensors to send physiological information to medical servers, allowing for the evaluation of a patient's condition [4]. These technologies can improve patient data processing and monitor and transmit pharmacological and medical information. This will help medical professionals make well-informed choices. Antennas are essential in this application to guarantee data transmission and reception.

UWB-enabled antennas have the potential to provide high data rates, low power consumption, and reliable performance in crowded frequency bands [5]. They are now a desirable choice for WBAN applications as a result of these [6-9]. The US Federal Communications Commission has designated the 3.1–10.6 GHz frequency range for UWB technology deployment. Unfortunately, UWB performance can be impacted by a number of narrow frequency bands that operate within these bands, such as the WLAN and WiMAX band. This may have an impact on transmission quality [9, 10]. As a result, there are many challenges in integrating UWB antennas in this application, chief among them being interference with existing communication systems and safety concerns around electromagnetic radiation absorption by the body [11]. Antennas are made with notched characteristics to block these undesirable narrow band signals because they can cause interference. A band-notch home has attracted a lot of attention lately. In recent years, a wide range of design methodologies have been used to comprehensively study numerous UWB antennas with band-notched properties [9-14]. Different shaped slots can be etched on the ground plane or radiating patch [15-17], electric resonators [18], split ring resonators [19], or complimentary-split-ring resonators [20], parasitic elements [21], and electromagnetic band gap (EBG) [8, 9] in order to achieve the notched characteristics with UWB antennas. Current UWB antennas for WBAN applications [22, 23] have limitations in terms of bandwidth, size, and high SAR. For WBAN applications, this study offers a compact UWB antenna with notched frequency and a lower SAR.

2. METHODS

The conventional antenna expressions were used in the antenna's design. Using the transmission line model, the patch's width and length were evaluated. The principle of size optimization included into the HFSS software was used to optimize the geometrical sizes derived from these evaluations. Changes in the length, width, and gaps surrounding the patch for this structure were assessed using the HFSS software, and the parameter values were optimized. The unwanted frequency components within the UWB spectrum were eliminated through slot-notching techniques, resulting in a notched band spanning from 6.5 GHz to 7.9 GHz to suppress interference from services operating in the upper C-band region.

2.1. Design Equations

The proposed design utilizes an FR4 substrate measuring 27 mm × 26 mm with a substrate thickness of 1.6 mm. The width *W* and length *L* of the patch is estimated with Eq. (1) and Eq. (2) [24].

$$W = \frac{1}{2f_r\sqrt{\mu_0\epsilon_0}}\sqrt{\frac{2}{\epsilon_r+1}} = \frac{v}{2f_r}\sqrt{\frac{2}{\epsilon_r+1}} \tag{1}$$

$$L = \frac{1}{2f_r\sqrt{\epsilon_{eff}}} - 2\Delta L \tag{2}$$

Within Eqs. (1) and (2), ϵ_r , v, μ_0 and ϵ_0 denote the substrate dielectric constant, the speed of light in free space, the permeability of free space, and the permittivity of free space, respectively, whereas the resonant frequency f_r of the microstrip antenna is defined as a function of its physical length in Eq. (3) [7]:

$$f_r = \frac{1}{2L\sqrt{\mu_0\epsilon_0}\sqrt{\epsilon_r}} = \frac{v}{2L\sqrt{\epsilon_r}} \tag{3}$$

Considering that the physical patch length incorporates an additional length ΔL, the resulting effective length L_{eff} for the dominant mode, excluding fringing fields, is described by Eq. (4):

$$L_{eff} = L + 2\Delta L \tag{4}$$

As defined in Eq. (4), ΔL is a function of the effective dielectric constant ϵ_{eff} and the substrate aspect ratio $(\frac{w}{h})$, expressed as:

$$\frac{\Delta L}{h} = 0.412\frac{(\epsilon_{eff}+3)\left(\frac{W}{h}+0.264\right)}{(\epsilon_{eff}-0.258)\left(\frac{W}{h}+0.8\right)} \tag{5}$$

The ε_{eff} of the substrate was calculated using Eq. (6) [8]:

$$\epsilon_{eff} = \frac{\epsilon_r+1}{2} + \frac{\epsilon_r-1}{2}\left[1+12\frac{h}{W}\right]^{-1/2} \tag{6}$$

and $\frac{w}{h} \gg 1$ represents the ratio of the substrate width to its height, which is used to reduce fringing effects. As previously stated, band notch rejection was achieved by cutting slots on the patch. The frequency of the notch was estimated using Eq. (7) [25]:

$$f_{notch(slot)} = \frac{V}{2\times l_{slot}\times\sqrt{\epsilon_{eff}}} \tag{7}$$

The height *h* of the patch and the feedline location was estimated using Eq. (8) to Eq. (10).

$$h = \frac{0.3\ x\ c}{2\pi f\sqrt{\epsilon_r}} \tag{8}$$

$$Y_f = \frac{W}{2} \tag{9}$$

$$X_f = \frac{L}{2\sqrt{\epsilon_{eff}}} \tag{10}$$

where X_f and Y_f are the feed points location along X-Y coordinates.

2.2. Antenna Geometry and Parametric Analysis

In this study, the length and width of the radiating patch, the length and shape of the ground plane as well as the feedline were optimized via the Genetic algorithm embedded within the HFSS software. The geometrical structure of the optimized antenna design is displayed in Figure 2. Numerous simulations were performed on the calculated dimensions, varying by 0.1 mm per simulation, in order to arrive at this size and shape. The ideal dimensions of 27 mm by 26 mm with a patch radius of 12 mm produced the best results. Additionally, the size of the H and U slots (Figure 2(c)) was varied until the desired frequency was notched. Table 1 displays the results of the sizing simulations using optimized geometry (Figure 2(b)). The antenna achieved a return loss of at least -10 dB in the frequency range of 3.4 GHz to 12.9 GHz, according to Figure 2(d). The antenna is appropriate for UWB applications because it has a bandwidth of 9.5 GHz. Additionally, as indicated by poin Fig. 2(d), the frequency range from 6.5 to 7.9 GHz was effectively notched, as evidenced by return loss values exceeding −10 dB within this band.

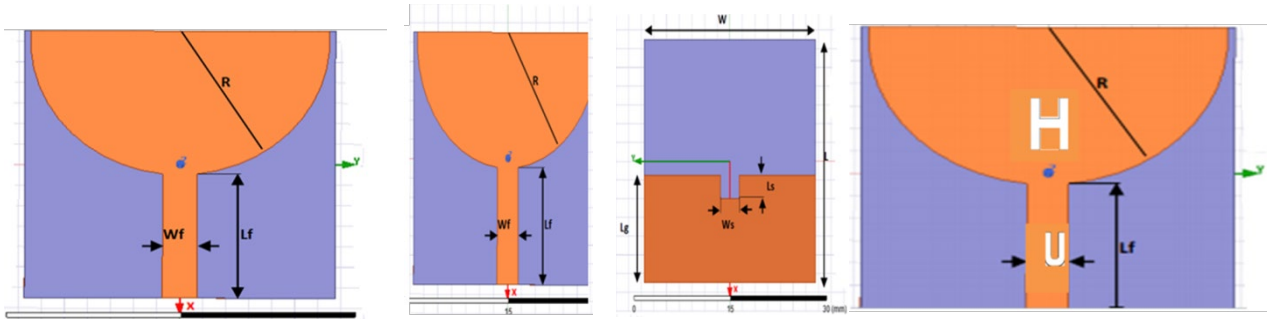

Figure 2. (a) Antenna patch and feedline, (b) optimized geometry of the UWB antenna, (c) UWB antenna with *U* and *H* slots (d) the S_{11} parameter of the antenna.

Table 1. Physical Parameters of the Proposed Antenna

Parameter	Value (mm)
Radius of patch (R)	12
X position (X_p), Y position (Y_p) of patch	-12 , 0
Length of substrate (L)	27
Width of substrate (W)	26
Partial ground plane (L_p)	11.5
Width feed line (W_f)	3
Length feed line (L_f)	13
Length of DGS slot (L_s)	3
Width of DGS slot (W_s)	4
Width of U slot (W_{Us})	5
Length U slot (W_{Us})	4.45
Length of H slot (L_{Hs})	6.4
Width of H slot (W_{Hs})	7.77
Gap between patch and insert feed G_{PF}	1
Input impedance	50 Ω

2.3. Performance Evaluation

A comprehensive evaluation of the antenna was carried out based on the S_{11} parameter, VSWR, surface current density, Poynting vector distribution, SAR, and group delay analysis. The S_{11} parameter expresses the proportion of the input signal that is reflected back from the antenna port. Moreover, it indicates the impedance matching between the radiating patch and the feeding line. The S_{11} parameter was calculated using Eq. (11).

$$S_{11} = 20\log\left(\left|\Gamma\right|\right) \tag{11}$$

where Γ denotes the reflection coefficient determined by

$$\Gamma = \frac{Z - Z_0}{Z + Z_0} \tag{12}$$

In Eq. (12), Z is the input impedance of the antenna while Z_0 is the characteristic impedance. The VSWR of the antenna was estimated using Eq. (13):

$$VSWR = \frac{1 + \Gamma}{1 - \Gamma} \tag{13}$$

The Poynting vector describes the flow of electromagnetic energy per unit area. This was estimated using Eq. (14):

$$\vec{S} = \frac{1}{\mu_0}\vec{E} \times \vec{H} \tag{14}$$

where $\vec{E}$ and $\vec{H}$ are the electric and magnetic field intensity respectively. The SAR calculates how much radiofrequency energy is absorbed by human tissue following transmission from the antenna. It is computed by averaging a specific volume, often one or ten grams of tissue. Eq. (15) [26] was used to estimate the SAR:

$$SAR = \int_s \frac{\sigma(r)|E(r)|^2}{\rho(r)} dr \tag{15}$$

where σ is the electrical conductivity and ρ is the mass density of the tissue, and E is the induced E-field radiated from the antenna.

3. RESULTS AND DISCUSSIONS

Figure 3 shows the VSWR plot for the UWB antenna. As shown in Figure 3, VSWR value of the antenna is lower than 2 in the operating frequency except in notched band, which one indicates efficient power transfer and broadband performance. In the notching-band VSWR values increases suddenly, and shows strong impedance mismatch effectively suppresses unwanted frequency components.

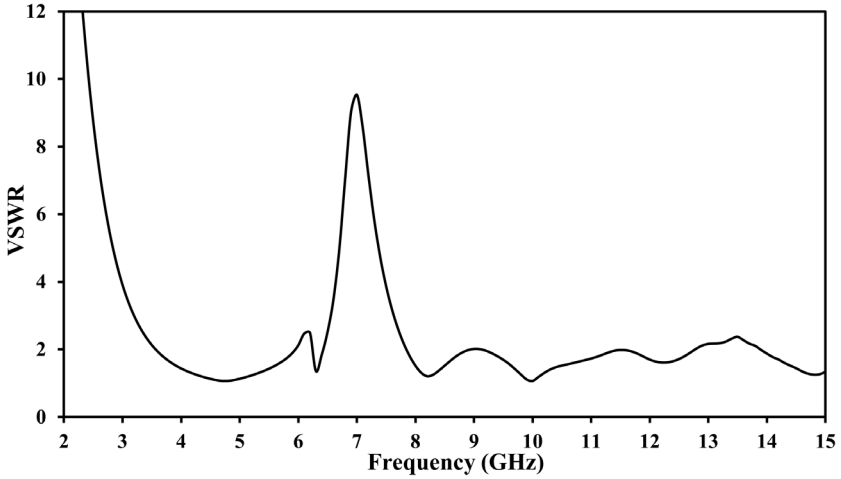

Figure 3. VSWR plot of the antenna.

Figure 4 shows the surface current distribution. From Figure 4, the feedline has an average current density of 62.68 A/m^2 and the radiating patch has an average surface current distribution of 42.38 A/m^2. This is an indication of high surface current density, the strong and well-distributed current on the radiating patch and feedline confirms efficient excitation and radiation at the frequency being simulated, which is ideal for a body centric UWB antenna.

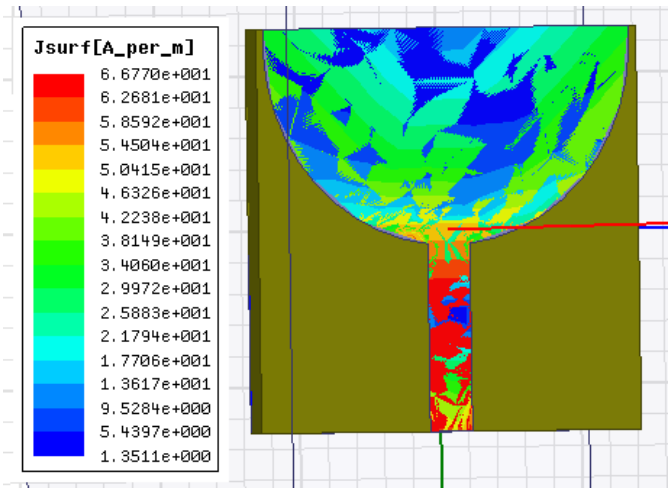

Figure 4. Surface current distribution of the antenna.

Figure 5 shows the Poynting vector plot for the UWB antenna. Figure 5 shows average Poynting value of 4.09 W/m^2 that is evenly distributed over the patch and the feedline of the antenna, this show a uniform radiated power density of the antenna. The value also conforms with safe limit of the FCC safety limit which is 5.8 W/m$^{2.}$. This shows that the antenna is safe to be deployed for WBAN applications.

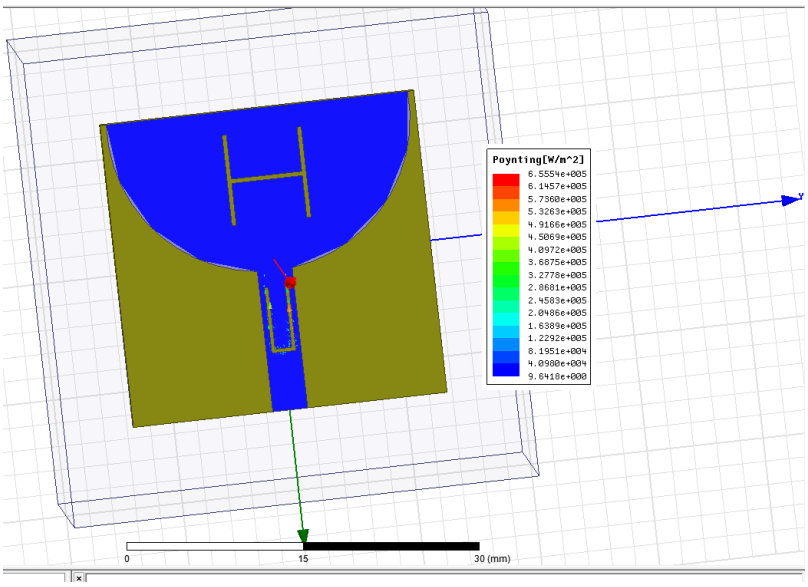

Figure 5. Poynting distribution plot of the antenna.

The normalized radiation patterns of the UWB antenna for 4 GHz and 9 GHz are given in Fig. 6, respectively. The antenna demonstrates an almost omnidirectional radiation behavior in the H-plane at 4 GHz, which is desirable for UWB communication systems, in addition, the E-plane pattern shows slight variations due to the finite ground plane and substrate effects at the 4 GHz; however, stable radiation behavior is maintained. The radiation pattern of 9 GHz is compared with the 4 GHz, it is evident that radiation pattern becomes more directive and exhibits multiple lobes due to higher-order resonant modes and increased electrical size of the antenna. It can be said that the antenna maintains stable radiation characteristics without deep nulls in the main radiation directions at the higher frequencies.

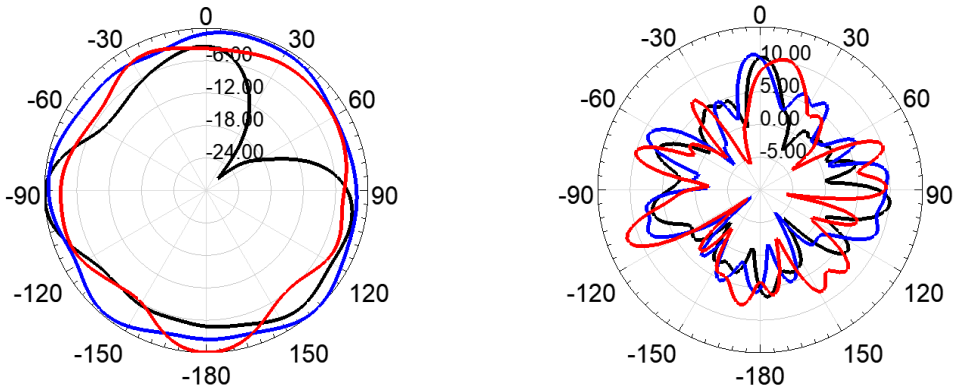

(a) 4 GHz (b) 9 GHz

Figure 6. The normalized radiation patterns of the antenna.

Figure 7 depicts the frequency-dependent variation of the antenna gain. The results show an increasing gain trend with frequency, except in the notching band. In the notching band the gain is decreasing suddenly. Outside the notched band, the gain is increasing again, and after the 9 GHz, it has a nearly stable value.

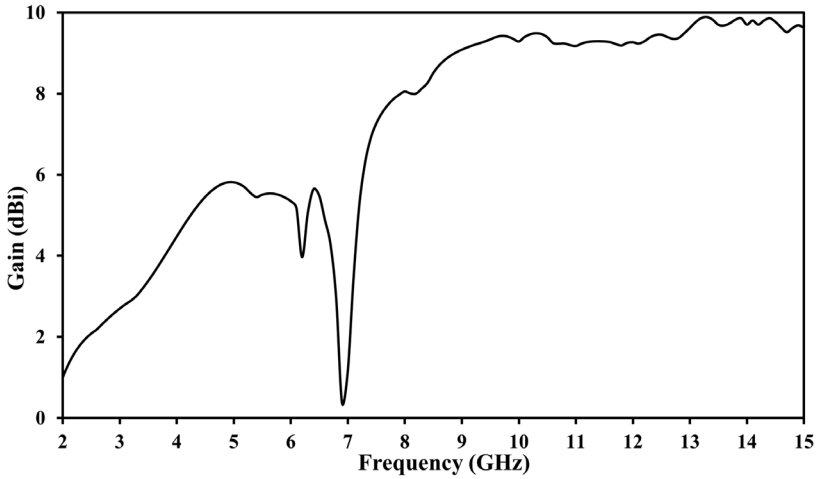

Figure 7. Antenna peak gain versus frequency.

Figure 8 shows the group delay plot of the band notched UWB antenna across the frequency band. The plot describes the time it takes for a signal to pass through an antenna and show the level of signal distortion along with phase. Variations in group delay across the frequency band can distort the signal, which ultimately influences the overall antenna performance. The Figure 8 shows a linear characteristic except at the notched frequency.

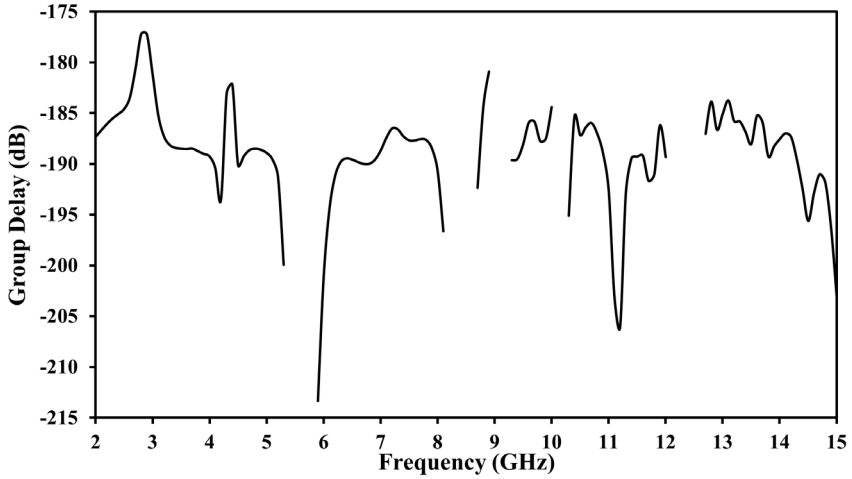

Figure 8. Group Delay Response of the UWB Antenna

To determine the radiation safety level for the human body, SAR analysis of the antenna was examined. Figure 9 displays the results of the analysis using a human phantom. It can be observed that SAR reduction was significantly improved by the designed antenna, averaging 0.8 W/kg across one gram of tissue. Compared to earlier research, which produced average values much above 2.06 W/kg [27], the results demonstrated a notable improvement. The FCC averages 1.6 W/Kg over one gram of tissue as the optimum value for body-centric antennas. This demonstrates that the low SAR UWB antenna developed in this study is appropriate for WBAN applications.

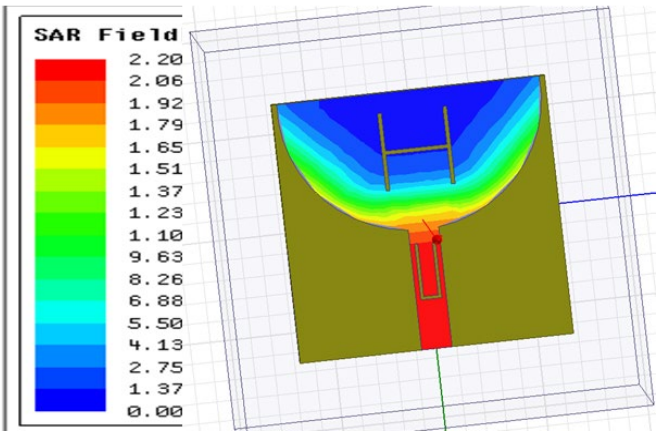

Figure 9. SAR field plots with human phantom.

Table 2 provides a comparison of the designed antenna with previously reported studies in the WBAN application domain. As can be observed, the current study has size advantages over others. Additionally, a superior performance is observed when the radiation level is considered.

Table 2. Comparison with other related studies under WBAN applications.

Author	Description	Size (mm^2)	SAR	Gain (dBi)	Bandwidth (GHz)
Chaturvedi and Raghavan [28]	The quarter-mode SIW antenna for on-body implementation using pork tissue as the biological phantom.	51 × 45	1 W/Kg for 1g mass of tissues	N/A	N/A
Anbalagan et al. [29]	A wearable textile antenna for ISM application.	51 × 45	0.486 10g of tissue	4.34	N/A
Alhawari et al. [30]	A Metamaterial-Inspired Flexible Elliptical UWB Antenna for WBAN and Breast Imaging Applications.	N/A	2 W/kg for 1g mass of tissues	Directional gain of 8.85 dB	N/A
Aruna et al. [31]	A flexible planar quasi-Yagi UWB antenna was designed for WBAN	34 × 52.3	N/A	7	7.4
This study	Band-notched UWB antenna for WBAN.	26 × 27	0.8 W/kg for 1g mass of tissues	6.4	3.4 – 12.9

N/A: Not available

4. CONCLUSION

Demand for WBAN has skyrocketed for a number of applications, such as personal entertainment, healthcare systems, sports monitoring, military services, and ambient intelligence. The capacity to send signals with an inherent noise-like behavior, a decreased risk of detection and intercept, and the potential for high data rates over short distances are some of the benefits of UWB technology over WBAN in these applications. However, the effectiveness of UWB technology is significantly impacted by interference from other narrow band signals. In this study, an antenna with band-notched feature is developed to reject interferences from two narrow band signals. In addition, since the antenna is intended for WBAN application, the designed antenna is compact with low SAR. The antenna design and analysis were carried out using the HFSS simulation tool. The simulation results revealed that a good performance is achieved in terms of the bandwidth, gain and SAR among others.

Acknowledgment

The authors wish to appreciate the management of the Federal University of Technology Akure for the opportunity given to conduct this research.

REFERENCES

[1] Olatinwo DD, Abu-Mahfouz A, Hancke G. A Survey on LPWAN Technologies in WBAN for Remote Health-Care Monitoring. Sensors. 2019;19(23):5268. doi:10.3390/s19235268

[2] Taleb H, Nasser A, Andrieux G, Charara N, Motta Cruz E. Wireless technologies, medical applications and future challenges in WBAN: a survey. Wireless Networks. 2021;27(8):5271-95. doi:10.1007/s11276-021-02780-2

[3] Yaghoubi M, Ahmed K, Miao Y. Wireless Body Area Network (WBAN): A Survey on Architecture, Technologies, Energy Consumption, and Security Challenges. Journal of Sensor and Actuator Networks. 2022;11(4):67. doi:10.3390/jsan11040067

[4] Bangash J, Abdullah A, Anisi M, Khan A. A Survey of Routing Protocols in Wireless Body Sensor Networks. Sensors. 2014;14(1):1322-57. doi:10.3390/s140101322

[5] Çelik K. A novel asymmetric antipodal Vivaldi MIMO antenna. AEU-International Journal of Electronics and Communications. 2024;187:155529. doi:10.1016/j.aeue.2024.155529

[6] Ahmad J, Hashmi M, Bakytbekov A, Falcone F. Design and Analysis of a Low Profile Millimeter-Wave Band Vivaldi MIMO Antenna for Wearable WBAN Applications. IEEE Access. 2024;12:70420-33. doi:10.1109/access.2024.3401865

[7] Douhi S, Zakaria Z, Idiri M, Eddiai A. Design and Simulation of a Flexible UWB MIMO Antenna for mm-Wave IoT Applications: Performance and SAR Evaluation. Advanced Theory and Simulations. 2025;8(9). doi:10.1002/adts.202500075

[8] Fadehan G, Olasoji YO, Adedeji KB. Development of a Triple Band Notched UWB Antenna. International Journal of Engineering Research in Africa. 2023;63:97-118. doi:10.4028/p-525842

[9] Fadehan GA, Olasoji YO, Adedeji KB. Frequency and Time Domain Analysis of Hybrid Triple-band-notched UWB Antenna. Transactions on Electromagnetic Spectrum. 2024;3(1):20-33. doi:10.5281/zenodo.8269702

[10] Radhakrishnan R, Gupta S. Metasurface-inspired circularly polarized patch antenna using DGS for sub 6-GHz applications. Journal of Electromagnetic Waves and Applications. 2024;38(6):639-51. doi:10.1080/09205071.2024.2321286

[11] Zhao L, Wang Y, Liu C, Song D, Hu C, Li C, et al. Compact Circular-Shaped MIMO Antenna Covers UWB Bandwidth With Four Frequently-Used Band-Notched Characteristics for Multi-Scenario Applications. IEEE Access. 2024;12:32762-71. doi:10.1109/access.2024.3371571

[12] Abbas A, Awan WA, Hussain N, Choi D, Lee S, Kim N. Highly selective-notch band ultrawide band antenna: A review. Heliyon. 2025;11(2):e41922. doi:10.1016/j.heliyon.2025.e41922

[13] Gautam AK, Yadav S, Rambabu K. Design of ultra-compact UWB antenna with band-notched characteristics for MIMO applications. IET Microwaves, Antennas & Propagation. 2018;12(12):1895-900. doi:10.1049/iet-map.2018.0012

[14] Yadav S, Gautam AK, Kanaujia BK. Design of dual band-notched lamp-shaped antenna with UWB characteristics. International Journal of Microwave and Wireless Technologies. 2015;9(2):395-402. doi:10.1017/s1759078715001609

[15] Srivastava G, Mohan A. Compact MIMO Slot Antenna for UWB Applications. IEEE Antennas and Wireless Propagation Letters. 2016;15:1057-60. doi:10.1109/lawp.2015.2491968

[16] Altaf A, Iqbal A, Smida A, Smida J, Althuwayb AA, Hassan Kiani S, et al. Isolation Improvement in UWB-MIMO Antenna System Using Slotted Stub. Electronics. 2020;9(10):1582. doi:10.3390/electronics9101582

[17] Çelik K. A novel band notched circular ring quad port UWB MIMO antenna. Sādhanā. 2025;50(3):154. doi:10.1007/s12046-025-02764-4

[18] Vendik IB, Rusakov A, Kanjanasit K, Hong J, Filonov D. Ultrawideband (UWB) Planar Antenna with Single-, Dual-, and Triple-Band Notched Characteristic Based on Electric Ring Resonator. IEEE Antennas and Wireless Propagation Letters. 2017;16:1597-600. doi:10.1109/lawp.2017.2652978

[19] Chakraborty M, Pal S, Chattoraj N. Quad notch UWB antenna using combination of slots and split-ring resonator. International Journal of RF and Microwave Computer-Aided Engineering. 2019;30(3). doi:10.1002/mmce.22086

[20] Kim D-O, Jo N-I, Jang H-A, Kim C-Y. Design of the Ultrawideband Antenna With a Quadruple-Band Rejection Characteristics Using a Combination of the Complementary Split Ring Resonators. Progress In Electromagnetics Research. 2011;112:93-107. doi:10.2528/pier10111607

[21] Marzouk M, Nejdi IH, Rhazi Y, Saih M, Nasir JA, Daher A, et al. Low-profile Reconfigurable UWB Fractal Antenna Enhanced by Parasitic Elements for Wireless Applications. Progress In Electromagnetics Research Letters. 2025;126:37-48. doi:10.2528/pierl25040402

[22] Abbasi QH, Rehman MU, Yang X, Alomainy A, Qaraqe K, Serpedin E. Ultrawideband Band-Notched Flexible Antenna for Wearable Applications. IEEE Antennas and Wireless Propagation Letters. 2013;12:1606-9. doi:10.1109/lawp.2013.2294214

[23] Irshad Khan M, Khattak MI, Rahman SU, Qazi AB, Telba AA, Sebak A. Design and Investigation of Modern UWB-MIMO Antenna with Optimized Isolation. Micromachines. 2020;11(4):432. doi:10.3390/mi11040432

[24] Dilruba Geyikoglu M. A novel UWB flexible antenna with dual notch bands for wearable biomedical devices. Analog Integrated Circuits and Signal Processing. 2023;114(3):439-50. doi:10.1007/s10470-023-02146-y

[25] Shrimal S, Agrawal R, Sharma IB, Garg J, Sharma MM. A Reconfigurable Multi-Band Notched Semi-Circle Engraved UWB Antenna for Wireless Applications. Scientia Iranica. 2024;0(0):0-. doi:10.24200/sci.2024.63713.8548

[26] Rekha S, Let GS. Design and SAR Analysis of Wearable UWB MIMO Antenna with Enhanced Isolation Using a Parasitic Structure. Iranian Journal of Science and Technology, Transactions of Electrical Engineering. 2022;46(2):291-301. doi:10.1007/s40998-022-00482-9

[27] Jayant S, Srivastava G, Purwar R. Bending and SAR analysis on UWB wearable MIMO antenna for on-arm WBAN applications. Frequenz. 2021;75(5-6):177-89. doi:10.1515/freq-2020-0105

[28] Chaturvedi D, Raghavan S. Circular Quarter-Mode SIW Antenna for WBAN Application. IETE Journal of Research. 2017;64(4):482-8. doi:10.1080/03772063.2017.1358115

[29] Anbalagan A, Sundarsingh EF, Ramalingam VS, Samdaria A, Gurion DB, Balamurugan K. Realization and Analysis of a Novel Low-Profile Embroidered Textile Antenna for Real-time Pulse Monitoring. IETE Journal of Research. 2020;68(6):4142-9. doi:10.1080/03772063.2020.1787877

[30] Alhawari ARH, Almawgani AHM, Hindi AT, Alghamdi H, Saeidi T. Metamaterial-based wearable flexible elliptical UWB antenna for WBAN and breast imaging applications. AIP Advances. 2021;11(1). doi:10.1063/5.0037232

[31] Aruna V, Alsath MGN, Kirubaveni S, Maheswari M. Flexible and Beam Steerable Planar UWB Quasi-Yagi Antenna for WBAN. IETE Journal of Research. 2019;68(3):2220-30. doi:10.1080/03772063.2019.1694453

